JACS
JOURNAL OF THE AMERICAN CHEMICAL SOCIETY

COMMUNICATION

pubs.acs.org/JACS

Electronic and Vibrational Signatures of the $Au_{102}(p\text{-MBA})_{44}$ Cluster

Eero Hulkko,[†] Olga Lopez-Acevedo,[†] Jaakko Koivisto,[†] Yael Levi-Kalisman,[‡] Roger D. Kornberg,[‡] Mika Pettersson,*[,†] and Hannu Häkkinen*[,†,§]

[†]Nanoscience Center, Department of Chemistry, P.O. Box 35, FI-40014 University of Jyväskylä, Finland

[‡]Department of Structural Biology, Stanford University School of Medicine, Stanford, California 94305, United States

[§]Nanoscience Center, Department of Physics, P.O. Box 35, FI-40014 University of Jyväskylä, Finland

Supporting Information

ABSTRACT: Optical absorption of a gold nanocluster of 102 Au atoms protected by 44 *para*-mercaptobenzoic acid (*p*-MBA) ligands is measured in the range of 0.05−6.2 eV (mid-IR to UV) by a combination of several techniques for purified samples in solid and solution phases. The results are compared to calculations for a model cluster $Au_{102}(SMe)_{44}$ based on the time-dependent density functional theory in the linear-response regime and using the known structure of $Au_{102}(p\text{-MBA})_{44}$. The measured and calculated molar absorption coefficients in the NIR−vis region are comparable, within a factor of 2, in the absolute scale. Several characteristic features are observed in the absorption in the range of 1.5−3.5 eV. The onset of the electronic transitions in the mid-IR region is experimentally observed at 0.45 ± 0.05 eV which compares well with the lowest calculated transition at 0.55 eV. Vibrations in the ligand layer give rise to fingerprint IR features below the onset of low-energy metal-to-metal electronic transitions. Partial exchange of the *p*-MBA ligand to glutathione does not affect the onset of the electronic transitions, which indicates that the metal core of the cluster is not affected by the ligand exchange. The full spectroscopic characterization of the $Au_{102}(p\text{-MBA})_{44}$ reported here for the first time gives benchmarks for further studies of manipulation and functionalization of this nanocluster to various applications.

Thiol-stabilized gold nanoclusters are robust particles that are currently under intense research owing to their fascinating size-dependent electronic, optical, chiroptical, photoluminescent, and bioconjugate properties.[1,2] Recent total-structure determinations of $Au_{102}(p\text{-MBA})_{44}$,[3] $Au_{25}(SPhC2)_{18}^{-1}$,[4,5] and $Au_{38}(SPhC2)_{24}$[6] clusters have shed light on the atomistic structure of the gold−thiolate interface and the nature of the surface-covalent Au−S bond. All these clusters have molecule-like electronic structures, with a stabilizing HOMO−LUMO gap that can be correlated to observed optical and/or electrochemical gaps.[7] Density functional theory has yielded insights into the electronic structure of these particles and has given predictions on their apparent energy gaps and specific shell closings of delocalized electrons in the gold core.[5,8−12]

Among the "generations"[13] (stable sizes) of the thiolate protected gold clusters in the mass range of 5−29 kDa, the cluster with the gold mass of about 21 kDa attracted special attention when the total-structure-determination of its water-soluble variant synthesized by using *p*-MBA thiols succeeded in 2007, yielding a definite assignment as $Au_{102}(p\text{-MBA})_{44}$.[3] The analysis of the structure revealed a central decahedral Au_{79} core protected by 19 RSAuSR and 2 $RS(AuSR)_2$ units (Supporting Information Figure S1).[3,9] Earlier computations by using density functional theory had predicted bonding motifs and compositions where Au^0 atoms form the metallic core and Au^I atoms are chemically bound in the protecting thiolate layer.[14]

Experimental data on optical or electrochemical gap of this cluster has not been available, mainly due to the fact that it was first obtained (and crystallized) from a mixture in which it was present in a trace amount.[3] However, a procedure that yields the compound in abundant, essentially pure form was very recently reported.[15] Here, we report, for the first time, a complete spectroscopic characterization of pure $Au_{102}(p\text{-MBA})_{44}$ samples in the spectral region of 0.05−6.2 eV (mid-IR to UV) by using a combination of several techniques in solid and solution phases, and study the electronic structure and electronic transitions by linear-response time-dependent density functional theory (LR-TDDFT). We will show the vibrational signatures of the *p*-MBA layer in the mid-IR region, give a definite demonstration of the quantum size effects in the electronic structure of this nanocluster by reporting the onset of electronic transitions in the NIR region where the calculated and measured absolute molar absorption agree quantitatively, and discuss signature features of absorption in the VIS region. Furthermore, we show that ligand exchange to glutathionate does not affect the electronic structure of the Au_{79} core.

$Au_{102}(p\text{-MBA})_{44}$ was synthesized as recently described.[15] Briefly, *p*-MBA and $HAuCl_4$ (3:1 ratio of *p*-MBA/gold) are combined in water and 47% methanol at a final gold concentration of 3 mM as follows: To 3.94 mL of water, we add 5.64 mL of methanol, 1.286 mL of 28 mM $HAuCl_4$ solution, and 1.134 mL of 95 mM *p*-MBA, 300 mM NaOH solution. The mixture is kept for 1 h at room temperature on a rocking platform. A total of 0.48 mL of 150 mM fresh $NaBH_4$ solution is added (2:1 ratio of BH_4^-:gold) and the reaction is allowed to proceed from a minimum of 5 h to as long as overnight at room temperature. The product is precipitated with ammonium acetate (80 mM final concentration) and methanol (80% v/v) and the pellet is then dissolved in a minimum amount of water. Further

Received: December 9, 2010
Published: February 24, 2011

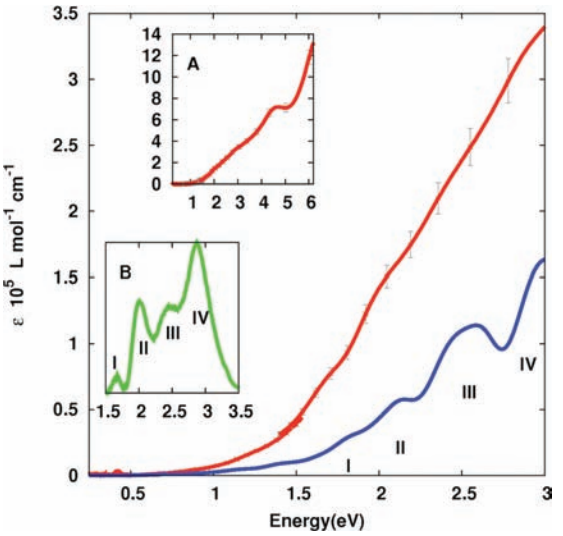

Figure 1. Absolute molar absorption coefficient of $Au_{102}(p\text{-MBA})_{44}$ (red curve) compared to the LR-TDDFT absorption spectrum of $Au_{102}(SMe)_{44}$ (blue). Inset A shows the full data up to 6.2 eV and inset B the baseline-corrected experimental spectrum in the region 1.5−3.5 eV. The feature at 4.5 eV in A is attributed to the *p*-MBA thiol.[15] Signature features in the vis range are labeled both in the experimental and theoretical spectra. The error bars in the red curves are determined based on estimation of uncertainty in concentration, optical path, and molar mass of the sample.

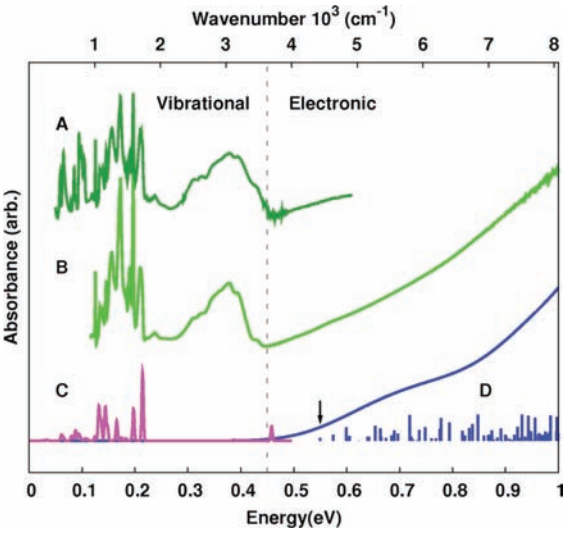

Figure 2. FTIR photoacoustic (A) and transmission (B) absorption spectra of the solid $Au_{102}(p\text{-MBA})_{44}$ samples, compared to (C) theoretical IR spectrum of a single *p*-MBA thiol and (D) LR-TDDFT absorption spectrum of $Au_{102}(SMe)_{44}$. The vertical gray line separates the approximate regions of vibrational and electronic transitions. The arrow indicates the lowest calculated electronic transition at 0.55 eV.

purification to get rid of contamination of larger clusters if formed is obtained by fractional precipitation with ammonium acetate (0.12 M final concentration) and methanol (60% v/v). The supernatant (pure $Au_{102}(p\text{-MBA})_{44}$) is then precipitated as described above and in ref 15.

Ligand exchange was performed by reacting equal volumes of $Au_{102}(p\text{-MBA})_{44}$ and glutathione (100 mM final concentration) for 1 h at 37 °C. Excess glutathione was removed by precipitation with ammonium acetate and methanol (as described above) and redissolved in water.

The liquid samples for spectroscopic experiments were prepared by dissolving solid material in H_2O or D_2O (c = 0.020−3 mM). Dry samples were prepared by placing a drop of solution on a CaF_2 window and letting the solvent evaporate leaving a thin film of dry material on the substrate. For photoacoustic measurements, the sample was dried in an aluminum cup. The spectra from the solution were measured with an FTIR spectrometer (Nicolet Magna 760) in the mid-IR to NIR region (1000−12 500 cm^{-1}) and with a UV/vis spectrometer (PerkinElmer Lambda 850) in the 200−900 nm region. The dry samples were measured in the mid-IR to NIR region (400−10 000 cm^{-1}) with an FTIR in transmission geometry or by using a photoacoustic detector (Gasera PA301).

Energy calculations and structure optimizations for the model cluster $Au_{102}(SMe)_{44}$, starting from the crystal structure of the $Au_{102}(p\text{-MBA})_{44}$,[3] were performed using the real-space finite-difference DFT code GPAW.[16] We used the outermost 11, 6, and 4 electrons as valence for Au, S, and C, respectively. GPAW uses the all-electron density, where the electrons are described using the projector augmented wave (PAW) method in the frozen core approximation. The PAW setup for Au($5d^{10}6s^1$) valence configuration included scalar-relativistic effects. Exchange and correlation effects were included through the Perdew, Burke, and Ernzerhof (PBE) energy functional.[17] The Kohn−Sham wave functions were expanded directly on a real space grid with a grid spacing of 0.2 Å. Optimizations of the considered structures were performed until the maximal force was below 0.05 eV/Å on any atom. LR-TDDFT calculations used the local density approximation for the kernel (with wave functions obtained from PBE). To compare to experiment, the absolute molar absorption coefficients were obtained by summing folded dipole moments and oscillatory strengths as explained in refs 11 and 18. The vibrational modes of a single *p*-MBA thiol were calculated from a finite difference approximation of the dynamical matrix and the IR intensities from a finite difference approximation of the gradient of the dipole moment.[19]

The absorption spectrum from the solution phase is shown in Figure 1 between 0.25 and 3 eV together with the calculated absorption spectrum. Inset A shows the data to 6.2 eV and inset B shows a portion of the experimental spectrum for which a baseline correction was done in order to highlight specific spectral features (labeled I to IV) in the region 1.5−3.5 eV. Measurement of this region with varying concentrations reproduced these features invariantly (see Supporting Information Figure S2). The overall agreement between the experimental and calculated spectrum up to 3 eV is nearly quantitative. The absolute molar absorption coefficient matches within a factor of 2 and the signature features in the 1.5−3.5 eV region are reproduced by the calculation (also labeled as I to IV). Both the experimental data and calculations indicate a band gap near 0.5 eV.

In spectra of liquid solutions, the solvent absorptions may mask the onset of the electronic transitions. To rectify this problem, the spectral region of the expected band gap was studied in more detail from the dry samples by using the FTIR. The experimental spectra are shown in Figure 2 together with the calculated absorption spectrum. Spectrum A was measured by the photoacoustic method, and spectrum B by FTIR in the transmission geometry from a thin film. Both data sets give a consistent result for the onset of electronic absorption at 0.45 ± 0.05 eV. More accurate

dx.doi.org/10.1021/ja111077e | *J. Am. Chem. Soc.* 2011, 133, 3752–3755

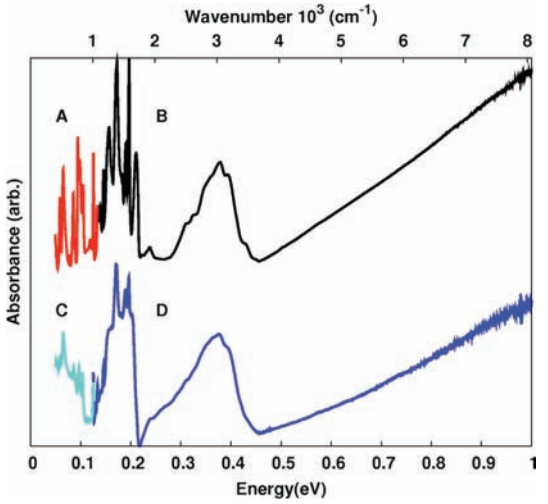

Figure 3. Comparison of IR absorption of the pure $Au_{102}(p\text{-MBA})_{44}$ (A and B) and glutahionate-exchanged Au_{102} clusters (C and D) in the mid-IR to NIR region. Data sets A and C originate from photoacoustic measurements and B and D are from transmission FTIR.

determination is hindered by the strong broad vibrational absorption feature around 0.4 eV. The absorption threshold is in a very good agreement with the calculation that predicts the lowest transition at 0.55 eV (spectrum D). Taking into account the bandwidth of the transition, the agreement with the experiment is excellent. Thus, we are able to establish here the onset of electronic absorption for the $Au_{102}(p\text{-MBA})_{44}$ cluster, unambiguously, for the first time.

The broad absorption feature at 0.3−0.45 eV region contains contributions from various vibrational transitions (Figure 2). The C−H and O−H groups of the ligand absorb in this region. In addition, some water is adsorbed on the clusters and various hydrogen bonding structures between water and carboxylic groups probably contribute to the broad bandwidth. Evidence of adsorbed water was obtained by observation of reversible changes in the band shape upon IR-irradiation in dry air atmosphere or upon pumping the sample to vacuum (Supporting Information Figure S3). The complicated structure with narrow peaks in the region 0.05−0.2 eV is due to vibrational fingerprint of the *p*-MBA ligand shell. Both transmission and photoacoustic spectra are similar in this region. Theoretical IR intensities for a single *p*-MBA thiol are shown in Figure 2 (data set C) and shown to match with the main experimental features in data sets A and B (see also Figure S4).

The ground state electronic structure of $Au_{102}(SR)_{44}$ (with SR = SMe or SR = *p*-MBA) has already been discussed before in the context of the superatom electronic structure model.[8,9] It was shown that the electronic structure is stabilized by an opening of an energy gap (HOMO−LUMO gap) of ≈0.5 eV at the shell-closing after 58 delocalized electrons in the gold core. The current data confirms this theoretical picture. The theoretical analysis (details shown in Figure S5) reveals that the lowest energy transitions just after the onset have predominantly Au(6sp) to Au(6sp) intraband character, with the onset of strong contributions from the Au(5d) band around 1.7 eV. This is consistent with earlier data on alkylthiolate-passivated Au clusters with core masses of ca. 14 kDa (70 Au atoms), 28−29 kDa (140−150 Au atoms), and 66 kDa where a "deflection point" (clear increase in the slope of the molar absorbance coefficient vs excitation energy) has been reported around 1.5−1.6 eV and interpreted as the onset of interband Au(5d) to Au(6sp) transitions.[13] Thus, it is interesting to note that the clusters even below 2 nm have the position of the upper edge of the Au(5d) band consistent with the band structure in the bulk.[20] However, finite-size effects are still manifested by the calculated and measured optical band gap of about 0.5 eV.

It is interesting to note here that no discernible HOMO−LUMO gap is reported from the electrochemical studies for the slightly larger nanocluster with 140−150 Au atoms,[7] which agrees with the theoretical determination of the electronic structure of the model cluster $Au_{144}(SR)_{60}$.[21] Consequently, the possible (meta)stable cluster sizes between Au_{102} and $Au_{140-150}$ should be interesting regarding the detailed studies of the disappearance of the band gap.

Figure 3 shows solid phase FTIR data on the pure $Au_{102}(p\text{-MBA})_{44}$ (upper curves A,B) compared to partially glutathionate-exchanged Au_{102} cluster (lower curves C,D). Three main obervations can be done: (i) differences in the vibrational spectrum confirm that ligand-exchange has occurred; (ii) the onset of electronic absorption is not affected by the ligand-exchange, indicating that the electronic shell structure of the Au_{79} core is not affected; and (iii) the ligand-exchange is not complete as evidenced by the remaining strong peaks characteristic of *p*-MBA.

The full spectroscopic characterization of $Au_{102}(p\text{-MBA})_{44}$ and $Au_{102}(p\text{-MBA})_{44-x}(SG)_x$ clusters facilitates further spectroscopic studies. The existence of the electronic band gap at about 0.5 eV suggests the possibility for luminescence in the IR region.[22] Rapid relaxation within the electronic manifold facilitates Raman spectroscopic studies as a further probe. Theoretical advancements shown here demonstrate the power of the LR-TDDFT to reliably yield absolute molar absorption coefficients for thiolate-protected gold clusters in a scale fully comparable to experiments.

■ ASSOCIATED CONTENT

Ⓢ Supporting Information. Structure of $Au_{102}(p\text{-MBA})_{44}$ (Figure S1), UV−vis spectrum at several concentrations (S2), additional data on shape of IR bands of the dry samples (S3), Figure 2 zoomed at low-energy region (S4), theoretical analysis of optical transitions of $Au_{102}(SMe)_{44}$ model cluster close to the band gap (S5), and the full citation to ref 16c. This material is available free of charge via the Internet at http://pubs.acs.org.

■ AUTHOR INFORMATION

Corresponding Author
mika.pettersson@jyu.fi; hannu.j.hakkinen@jyu.fi

■ ACKNOWLEDGMENT

This work is supported by the Academy of Finland and by NSF grant CHE 0750059 to R.D.K. The computations were done at CSC − the Finnish IT Center for Science in Espoo. We thank R. L. Whetten for useful discussions.

■ REFERENCES

(1) (a) Brust, M.; Walker, M.; Bethell, D.; Schiffrin, D. J.; Whyman, R. *Chem. Commun.* **1994**, 801.(b) Brust, M.; Kiely, C. J. *Colloids and*

Colloid Assemblies; Caruso, F., Ed.; Wiley-VCH: Weinheim, Germany, 2004; p 96.

(2) (a) Daniel, M. C.; Astruc, D. *Chem. Rev.* **2004**, *104*, 293. (b) Murray, R. W. *Chem. Rev.* **2008**, *108*, 2688. (c) Ackerson, C. J.; Jadzinsky, P. D.; Sexton, J. Z.; Bushnell, D. A.; Kornberg, R. D. *Bioconjugate Chem.* **2010**, *21*, 214–218.

(3) Jadzinsky, P. D.; Calero, G.; Ackerson, C. J.; Bushnell, D. A.; Kornberg, R. D. *Science* **2007**, *19*, 430–433.

(4) Heaven, M. W.; Dass, A.; White, P. S.; Holt, K. M.; Murray, R. W. *J. Am. Chem. Soc.* **2008**, *130*, 3754.

(5) Zhu, M.; Aikens, C. M.; Hollander, F. J.; Schatz, G. C.; Jin, R. *J. Am. Chem. Soc.* **2008**, *130*, 5883.

(6) Qian, H.; Eckenhoff, W. T.; Zhu, Y.; Pintauer, T.; Jin., R. *J. Am. Chem. Soc.* **2010**, *132*, 8280.

(7) (a) Hicks, J. F.; Miles, D. T.; Murray, R. W. *J. Am. Chem. Soc.* **2002**, *124*, 13322. (b) Quinn, B. M.; Liljeroth, P.; Ruiz, V.; Laaksonen, T.; Kontturi, K. *J. Am. Chem. Soc.* **2003**, *125*, 6644.

(8) Häkkinen, H. *Chem. Soc. Rev.* **2008**, *37*, 1847.

(9) Walter, M.; Akola, J.; Lopez-Acevedo, O.; Jadzinsky, P. D.; Calero, G.; Ackerson, C. J.; Whetten, R. L.; Grönbeck, H.; Häkkinen, H. *Proc. Natl. Acad. Sci. U.S.A.* **2008**, *105*, 9157–9162.

(10) Akola, J.; Walter, M.; Whetten, R. L.; Häkkinen, H.; Grönbeck, H. *J. Am. Chem. Soc.* **2008**, *130*, 3756.

(11) Lopez-Acevedo, O.; Tsunoyama, H.; Tsukuda, T.; Häkkinen, H.; Aikens, C. M. *J. Am. Chem. Soc.* **2010**, *132*, 8210.

(12) (a) Aikens, C. M. *J. Phys. Chem. C* **2008**, *112*, 19797. (b) Li, Y.; Galli, G.; Gygi, F. *ACS Nano* **2008**, *2*, 1896. (c) Gao, Y.; Shao, N.; Zeng, X. C. *ACS Nano* **2008**, *2*, 1497. (d) Reimers, J. R.; Wang, Y.; Cankurtaran, B. O.; Ford, M. J. *J. Am. Chem. Soc.* **2010**, *132*, 8378.

(13) (a) Schaaff, T. G.; Whetten, R. L. *J. Phys. Chem. B* **2000**, *104*, 2630. (b) Bigioni, T. P.; Whetten, R. L.; Dag, Ö. *J. Phys. Chem. B.* **2000**, *104*, 6983. (c) Schaaff, T. G.; Shafigullin, M. T.; Khoury, J. T.; Vezmar, I.; Whetten, R. L. *J. Phys. Chem. B* **2001**, *105*, 8785. (d) Wyrwas, R. B.; Alvarez, M. M.; Khoury, J. T.; Price, R. C.; Schaaff, T. G.; Whetten, R. L. *Eur. Phys. J. D* **2007**, *43*, 91. (e) Bradshaw, J. Ph.D. Thesis, Georgia Institute of Technology 2008 (see http://smartech.gatech.edu/handle/1853/26512).

(14) Häkkinen., H.; Walter, M.; Grönbeck, H. *J. Phys. Chem. B* **2006**, *110*, 9927.

(15) Levi-Kalisman, Y.; Jadzinsky, P. D.; Kalisman, N.; Tsunoyama, H.; Tsukuda, T.; Bushnell, D. A.; Kornberg, R. D. *J. Am. Chem. Soc.* **2011**, *133*, 2976–2982.

(16) (a) Mortensen, J. J.; Hansen, L. B.; Jacobsen, K. W. *Phys. Rev. B* **2005**, *71*, 035109. (b) Walter, M.; Häkkinen, H.; Lehtovaara, L.; Puska, M.; Enkovaara, J.; Rostgaard, C.; Mortensen, J. J. *J. Chem. Phys.* **2008**, *128*, 244101. (c) Enkovaara, J.; et al. *J. Phys. Cond. Matt.* **2010**, *22*, 253202. The code can be downloaded at https://wiki.fysik.dtu.dk/gpaw.

(17) Perdew, J. P.; Burke, K.; Ernzerhof, M. *Phys. Rev. Lett.* **1996**, *77*, 3865–3868.

(18) Schellman, J. A. *Chem. Rev.* **1974**, *75*, 323–331.

(19) Porezag, D.; Peterson, M. R. *Phys. Rev. B* **1996**, *54*, 7830.

(20) Opahle, I. Ph.D. Thesis, TU Dresden, 2001. http://www.ifw-dresden.de/institutes/itf/diploma-and-phd-theses-at-the-itf/ingo_opahle_phd.pdf/view

(21) Lopez-Acevedo, O.; Akola, J.; Whetten, R. L.; Grönbeck, H.; Häkkinen, H. *J. Phys. Chem. C* **2009**, *113*, 5035.

(22) (a) Miller, S. A.; Womick, J. M.; Parker, J. F.; Murray, R. W.; Moran, A. M. *J. Phys. Chem. C* **2009**, *113*, 9440. (b) Varnavski, O.; Ramakrishna, G.; Kim, J.; Lee, D.; Goodson, T. *J. Am. Chem. Soc.* **2010**, *132*, 16. (c) Yau, S. H.; Varnavski, O.; Gilbertson, J. D.; Chandler, B.; Ramakrishna, G.; Goodson, T. *J. Phys. Chem. C* **2010**, *114*, 15979.